공학석사학위논문

Activity Enhancement of *Bacillus circulans* Xylanase by Modulating Flexibility of Hinge Region

경첩 지역의 유연성 조작을 통한 *Bacillus circulans* 자일라네이즈의 활성도 증진

2012년 8월

서울대학교 대학원

협동과정 바이오엔지니어링 전공

FUKURA KAZUYO

Abstract

Enzymes are dynamic molecules which undergo multiple conformational changes in the solution, and the dynamics is considered to play a critical role in enzyme activity. Hinge bending motions are known to be related with turnover rate, which result from relative movements of dynamical quasi-rigid bodies and the motions are affected by the physical properties of the hinge region. In this study, hinge identification and flexibility modification of that region by mutagenesis were conducted to explore the relationship between the hinge flexibility and activity. *Bacillus circulans* xylanases was used to identify the hinge region and the target sites were selected in the region for mutagenesis. As a result, turnover rate (V_{max}) was improved about two folds in the mutant substituted to be more rigid structure. This study indicates the importance of hinge flexibility and the rigidly mutated hinge has positive effects to the enzyme activity.

Keywords: Protein, Activity, V_{max}, Dynamics, Flexibility, Hinge, Xylanase

Student number: 2010-23357

Contents

List of Figures

List of Tables

1. Introduction

Enzymes feature great advantages in terms of high selectivity, molecule conversion at ambient conditions, low energy consumption and low byproduct formation. Due to these features biocatalysis is esteemed as an environmentally friendly method for molecule synthesis and can lead to cost reduction in overall process [Sime, 1999]. Successful application of enzymes in the synthetic industry requires increased product titer and increased catalyst efficiency. There have been methods to enhance the biocatalyst efficiency such as enzyme screening, inhibitor removal, activator addition and protein engineering. Among the methods, protein engineering is regarded as the most suitable one to obtain the required enzyme improvement. For the enzyme engineering two broad approaches have been taken, namely directed evolution and rational design. Whereas the former takes random mutational strategy, the latter can obtain the required improvement on logical basis with the information such as structure and sequence. Rational design, therefore, is preferred to engineer protein if there is such information. However, there has been little research on rational design for the activity enhancement, especially general strategy known to date.

Enzymes are dynamic and flexible molecules exhibiting oscillating motions, which are known to be related with the catalytic function [Yon et al., 1998, Hammes, 2002]. Dynamical substructures have been taken notice due to the

subunit motions are observed in functional cycles of many enzymes [Schulz, 1991]. Flexibility of each part of enzyme contributed to maintaining dimensional structure and functional activity. Consequently it is desirable to analyze the pivot residues for exploring the flexibility-activity relationships. The pivot residues which act as mechanical hinge are defined the linker region between moving quasi-rigid bodies. The hinge region is consumed to have role in promoting or sustaining the conformational change required for catalysis **[**Schramm et al., 2008]. In functionally similar enzymes such as the hydrolases, the catalytic site is laid close to the interdomain region between the two quasi-rigid bodies [Potestio et al., 2009]. The position is influent for maintaining the geometry of the active site precisely, while allowing for a functionally-oriented modulation of the adjacent regions resulting from the relative two subunit motion.

Endo-1,4-β-xylanases (E.C.3.2.1.8) are endo-glycosidases which cleave the β-xylosidic bond between xylose residues. GH11 family assessing high selectivity and activity has accumulated numerous available sequences and three dimensional structures, which leads this family of enzyme to application in various biotechnological field such as biobleaching, food and feed [Coughlan et al., 1993]. GH11, its structure is analogous to a right hand (Figure 1), contains α-helix and two β-sheets forming β-sandwich. Both β-sheets represent twisted backbone and form the cleft where xylose residues bind. Two conserved glutamic acids as catalytic residues are on different side of the cleft. From crystal

structures, it is revealed that it conducts hinge bending motion during catalysis. Specifically *Bacillus circulans* xylanase was chosen as a target enzyme because of its plentiful information such as studied properties and crystallographic structures.

The goal of this work is to explore the relationship between the hinge flexibility and activity. The flexibility of hinge region was studied by site-directed mutagenesis of a few residues on or near the identified hinge region to elucidate the relationship between rigidity level and activity. The selected residues were substituted to several amino acids with different flexibility regarding B-factor profile of amino acids and the changes in intra-protein interactions.

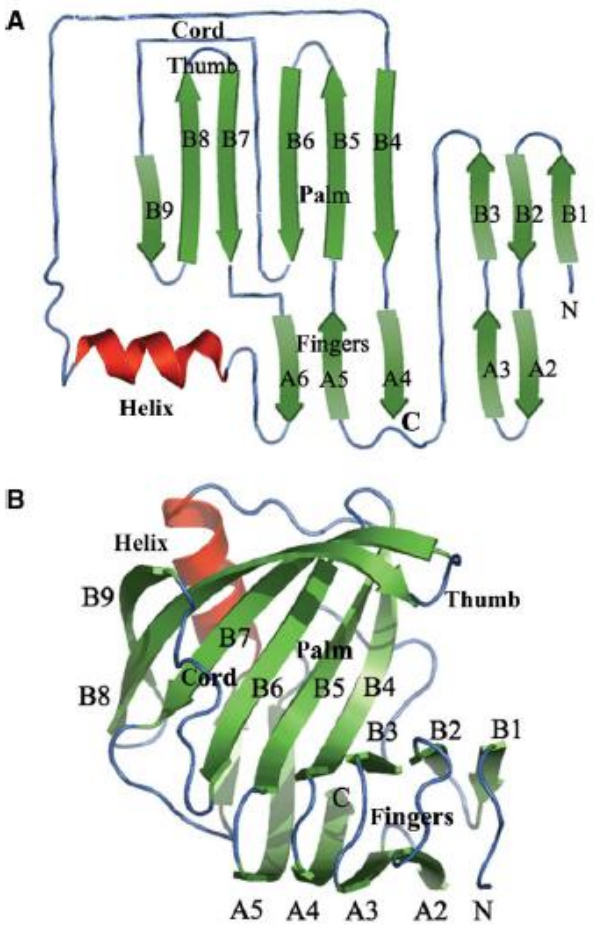

Figure 1. (A) Topology diagram and (B) a schematic 3D structure of the family 11 xylanases [Purmonen et al., 2007].

2. Theoretical background

2.1. Enhancement of enzyme activity

There have been several methods to increase enzyme efficiency which are briefly classified to two approaches, i.e. external and internal molecular methods. The former contains modification of the environment such as temperature and pH shift and inhibitor removal or activator addition. Screening of enzyme with high activity is also contained in the former method. The latter is protein engineering that alters the enzyme properties by mutagenesis of amino acid sequence, which allows the enzyme to obtain required properties in the given circumstance.

There are two representative strategies in the enzyme engineering, i.e. the directed evolution and the rational design. The directed evolution is carried out by random mutagenesis and screening of mutants with increased activity. On the other hand, the rational design is carried out based on the structural analysis using literature information and computational tools and generally site-directed mutagenesis is conducted to enhance the activity.

2.2. Dynamics, Flexibility and Enzymatic Catalysis

Enzyme exists as a dynamically active molecule [Neet, 1998] and its motions and intrinsic flexibility play critical roles in catalytic functionality [Yon et al., 1998, Hammes, 2002].

Enzymes consist of amino acid sequence connected by peptide bonds, where each atom is involved in interaction networks to maintain three-dimensional structure and there occur various scales of motions by exchange of labile protons [Kim et al., 1993]. The dynamic property allows intimately enzymes to do biological functions. Dynamics is used as intrinsic subregional motions not uniformly allocated throughout the enzyme and in terms of time scale, it is classified to three, atomic motions (10^{-15} to 10^{-1} s) including atomic fluctuations and side chain motions, rigid body motions (10^{-9} to 1 s) including helix, domain and subunit motions and large-scale motions (10^{-7} to 10^{4} s) [Brooks et al., 1998]. Among the three kinds of motions, the rigid body motion might directly be related with the substrate converting because the time scale of this motion and that of turnover rate are similar. In addition, the motions are responsible for altering the activation free energy barrier at the transition state [Hammes-Schiffer, 2002].

In terms of protein, flexibility represents the ability to adapt to different ligands

or environments. To describe the enzymatic catalytic mechanism, induced fit theory [Koshland, 1958] is broadly used as an appropriate model, rather than lock-and-key theory [Fischer, 1894]. In the theory an enzyme undergoes conformational changes induced by substrate binding and then there emerges a catalytic competence, which is suitable to explain catalytic cycle where enzyme-substrate collision, binding, chemical reaction and product release occur in order. The conformational change for stabilizing substrate binding and occurring efficient chemical reaction is manipulated by the pre-encoded flexibility, therefore it is indicated that enzyme flexibility directly contributes to its catalysis. Flexibility is also involved in enzyme folding and maintaining its conformation. As shown in Figure 2 (B), residual flexibility represented by B-factor is different from each residue, which is pre-assigned to maintain its proper folding and functionality. As information of the crystal structure becomes tremendous it is observed in a lot of proteins that there is conformational change between substrate free and bound structures.

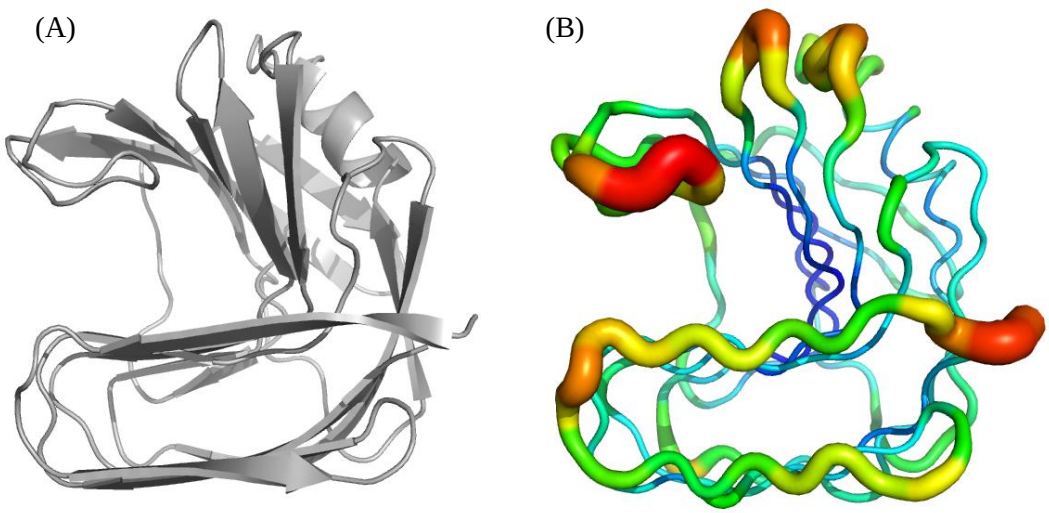

Figure 2. Crystallographic structures of *Bacillus circulans* xylanase (PDB ID : 1XNB) (A) Crystal structure represented by ribbon (B) Crystal structure represented by the level of B-factor in color and thickness

2.3. Hinge and catalysis

Considering function-dynamics relationship, there is growing interest in investigation of domain (or protein subunit) motions since in many proteins the motion is related with functionality [Schulz, 1991]. Such quasi-rigid bodies can move with respect to others while their own folds remain essentially unaffected. There occurs fixed boundary region between two motional subunits of a protein and the region is defined as a hinge in enzymes. The hinge region is observed in many enzymes exhibiting hinge-bending motion which altering the relative distance between large rigidly-moving regions.

The hinge bending motion plays a role in catalysis, i.e. maintaining the precise geometry of the active site, while allowing for an appreciable functionally-oriented modulation of the flanking regions resulting from the relative motion of the two sub-domains. Mutational investigation at the hinge region with human3-phosphoglycerate kinase (hPGK) implies several residues in the main hinge (β-strand) have roles in regulating domain movements and in maintaining the conformational coherence of the whole protein. In addition interactions of the side chains of the residues in the hinge might be in charge of the domain movement [Szabo et al., 2008]. In the study with human adenylate kinase 4, the mutant in the critical hinge region dramatically altered the moving direction of connected domains, provides an example that the domain is directly regulated by hinge without substrate binding [Tsuchiya et al., 2009].

3. Materials and Methods

3.1. Hinge identification

Hinge in enzyme is located in the divided region by two collective moving regions during dynamics or by comparing substrate free and bound forms. To detect the region meeting the requirements, computational tools of protein decomposition and that of hinge detection by comparing apo and substrate bound forms were introduced. The detected regions which overlap the results from each program were finally selected as a target hinge. There are substrate free and bound crystal structures of the model enzyme *Bacillus circulans* xylanase (*Bc*x); PDB ID: 1XNB and 1BVV respectively (RCSB Protein Data Bank; www.rcsb.org) and the structures were used to detect the hinge by the above method.

Protein decomposition

Protein decomposer PiSQRD was used to subdivide *Bc*x into several approximately-rigid units. The web resource groups amino acids in pre assigned number by pairwise distances between a set of two amino acids remain unaltered in the course of protein equilibrium fluctuations [Potestio et al., 2009]. The substrate free and bound forms, 1XNB and 1BVV were subdivided in a range of group number two to seven. After application in every pre assigned grouping

number, the boundary residues coinciding over five subdivisions are selected in the both structures. The overlapping residues in the two groups are finally chosen as the hinge region of *Bc*x.

Hinge detection

Hinge detector DynDom was used to identify hinge region of *Bc*x by comparing substrate free and bound structures. This software provides the information of domains, hinge axes and hinge bending residues of proteins as output where two conformations are submitted [Hayward et al., 2002]. The substrate free and bound structures of *Bacillus subtilis* xylanase as GH11 xylanases were used to detect the hinge region.

***in silico* mutation**

SCWRL4 was used to carry out *in silico* mutations for simulating the results of mutating target residues. The program predicts proper side chain conformation of substituted amino acid [Krivov et al., 2009]. In all selected sites, the mutations to the determined amino acids were performed via the computer simulation.

3.2. Flexibility analysis

B-factor profile of amino acids

The flexibility index of all kinds of amino acids was used to predict flexibility of a certain amino acid. The index correlates with tendency of the side chain to be buried or exposed, which provides information that a certain amino acid is likely to be rigid or flexible in the globular amino acid [Radivojac et al., 2004].

Intra-protein nteraction

Protein Interactions Calculator (PIC) was used to calculate interactions of the enzyme. This webserver identifies various kinds of interactions; such as disulphide bonds, hydrophobic interactions, ionic interactions, hydrogen bonds, aromatic-aromatic interactions, aromatic-sulphur interactions and cation-π interactions within a protein [Tina et al., 2007]. The structures *Bc*x and the mutants which generated by *in silico* mutation were used to recognize the internal interactions.

Residual flexibility

Floppy Inclusions and Rigid Substrate Topography (FIRST) and Framework Rigidity Optimized Dynamics Algorithm (FRODA) on the Flexweb server were used to calculate the residual flexibility of *Bc*x. FIRST is a software which identifies rigidity and flexibility in network graphs and then FRODA predict

dynamics according to the static results of the FIRST analysis [Wells et al., 2005]. The substrate free and bound structures 1XNB and 1BVV were calculated by momentum as a motion type until 5000 conformers are generated.

Table 1. Amino acid flexibility index [Radivojac et al., 2004]

Amino Acid [a]																			
W	C	F	I	Y	V	L	H	M	A	T	R	G	Q	S	N	P	D	E	K

[a] The order of the amino acids along the x-axis from left to right is the most buried (rigid) to the most exposed (flexible)

3.3. Biomolecular and chemical materials

The synthetic gene of *Bacillus circulans* xylanse (*Bc*x) was a generous gift from Department of Biochemistry and Molecular Biology, University of British Columbia. Restriction enzymes (*Nhe* I, *Xho* I and *Dpn* I) and P*fu* DNA polymerase were from NEB (Ipswich, USA) and Bioneer (Daejon, Korea), respectively. Competent *E.coli* strain Top10 and BL21 (DE3) were from Invitrogen (Carlsbad, CA, USA) and Novagen (Madison, WI, USA) respectively. Ni-NTA agarose for His-tag purification was from Qiagen (Valencia, CA, USA). BSA protein and dye reagent for protein assay were from Bio-RAD (Hercules, USA). Polymeric xylan substrate Beechwood xylan and xylose for product standard curve were from Sigma (St. Louis, USA).

3.4. Site-directed mutagenesis

The xylanase gene was PCR-amplified from the synthetic BCX gene. The amplified fragments were digested by *Nhe* I and *Xho* I and then cloned into the multi-cloning site of the pET-23b(+) vector (Novagen, USA) to produce the recombinant plasmid p23bBCX. Site-specific mutants were generated using the efficient primer design method describes by Lei Zheng et al. [Zheng et al., 2004] which is based on Quick-Change site-directed mutagenesis protocol [Fisher et al., 1997]. The synthesized primers for all mutants were listed Table 2. The PCR reaction mixture consists of the synthetic BCX gene (1ul) as template DNA, complementary designed primers (1ul for forward and reverse respectively), p*fu* DNA polymerase (1ul) and p*fu* buffer (47ul) in 50ul. The mixture was heated for PCR elongation (94℃ for 3min and then 1min, 52℃ for 1min, 68℃ for 10min (16x) and then 1 h). The PCR products were purified by PCR purification kit and incubated in restriction reaction with *Dpn* I at 37℃ for 2h. The restricted gene transformed to *E.coli* Top10 by heat shock (92 ℃ for 90 sec). The successfully transformed cells were selected by incubating on LB agar plate supplemented with 50ug/ml of ampicillin and then were cultured in LB media supplemented with 50ug/ml of amplicillin (3ml). The mutant plasmids were isolated for sequencing and the mutations were verified by Cosmogentech (Daejeon, Korea).

Table 2. Primers of all mutants

Enzymes	Tmeplate	Primers
Wild-type BCX	-	
V131S	p23bBCX	Forward: 5’ CAGTATTGGAGTAGTAGACAATCTAAGCGGCCGACTG 3’ Reverse: 5’ CGCTTAGATTGTCTACTACTCCAATACTGAGTAAAGG 3’
R132M	p23bBCX	Forward: 5’ CAGTATTGGAGTGTTATGCAATCTAAGCGGCCGACTG 3’ Reverse: 5’ CGCTTAGATTGCATAACACTCCAATACTGAGTAAAGG 3’
R132L	p23bBCX	Forward: 5’ CAGTATTGGAGTGTTTTACAATCTAAGCGGCCGACTG 3’ Reverse: 5’ CGCTTAGATTGTAAAACACTCCAATACTGAGTAAAGG 3’
N141G	p23bBCX	Forward: 5’ GTTCGGGCGCCACCATTACGTTCACCAATCAC 3’ Reverse: 5’ GTGGCGCCCGAACCAGTCGGCCGCTTAGATTG 3’
N141T	p23bBCX	Forward: 5’ GACTGGTTCGACCGCCACCATTACGTTCACCAATC 3’ Reverse: 5’ GTAATGGTGGCGGTCGAACCAGTCGGCCGCTTAG 3
N141V	p23bBCX	Forward: 5’ GACTGGTTCGGTCGCCACCATTACGTTCACCAATC 3’ Reverse: 5’ GTAATGGTGGCGACCGAACCAGTCGGCCGCTTAG 3’
A142I	p23bBCX	Forward: 5’ GACTGGTTCGAACATCACCATTACGTTCACCAATC 3’ Reverse: 5’ GTAATGGTGATGTTCGAACCAGTCGGCCGCTTAG 3’

3.5. Expression and purification of enzyme

The constructed plasmid was transformed into *E.coli* BL21 (DE3) by heat shock (92 ℃ for 90 sec). The transformants carrying genes of wild type and mutant xylanases were cultivated in LB media supplemented with 50ug/ml of ampicillin (3ml) at 37℃. 1mM IPTG was added at absorbance 0.4 ~ 0.6 at 600nm to induce the enzyme expression and cultivation was continued at 20℃ for 24 h. The expressed cells were isolated and were disrupted by sonication on ice and the supernatant containing the extracellular enzyme was separated from cell debris by centrifugation (8,000 rpm, 20 min).

Expressed xylanases were purified on a Ni-NTA agarose column. The supernatant was mixed with the Ni-NTA beads for at -4℃ for 1 h. Washing was conducted in a buffer containing 40mM imidazole and elution in a buffer containing 10mM imidazole. Enzyme purity was assessed by analysis on 12% SDS-PAGE. Determination of enzyme concentration was carried out by a modified Bradford assay [Bradford, 1976] according to the instructions of manufacture.

3.6. Enzyme activity and determination of kinetic parameters

Enzyme activity was assayed using modified dinitrosalicylic (DNS) acid method described by Bailey et al [Bailey et al., 1992] with Beechwood xylan as a substrate. The reaction mixture containing 100ng/ml enzyme (40ul) and 1% (w/v) xylan solution (360ul) was incubated at 40℃ for 5 min and DNS solution (600ul) was added to stop the reaction. The mixture was conducted to boiling and cooling for 2 min respectively. In this method the activity is assessed by measuring the release of oligosaccharides and reducing sugars which react with DNS acid. After the reaction the absorbance of the color developed mixture was measured at 540nm. One unit of xylanase activity was interpreted as the amount of enzyme required to generate 1umol of the reducing sugars in 1 min at 40℃ using xylose as a standard product.

Kinetic assay was carried out at 40℃ with substrate concentrations in the range of 0.05~1.2% (w/v) and the kinetic parameters (K_m and V_{max}) were calculated using the Lineweaver-Burk equation. All kinetic parameters are the mean of triplicate measurements.

4. Results and Discussion

4.1. Hinge region identification

Hinge regions were identified using computational tools, e.g. PiSQRD and DynDom and then the target hinge region was chosen as the consensus part detected by the both programs. As a result four hinge regions were identified and the two regions (127-130, 159-160) were at or near the putative hinge of the literature analyzing *Trichoderma reesei* xylanase [Muilu et al., 1998] when superimposing both the structures. The others were located in the hinge axes formed when comparing substrate bound and free conformatons. This result indicates that identification of hinge region is carried out with public program without a lot of information of crystallographic structures or other proteins in the same family. The result was analyzed by the fluctuation calculating webserver, FIRST (PRODA) (Figure 3).

In many cases more than one conformation was crystallized from a protein and from the structure in different states dynamical domains were observed. The domains might be defined as residual groups moving in a concerted mode [Hayward et al., 1998] and hinge regions exist between the domains. PiSQRD was run to decompose the model enzyme *Bacillus circulans* xylanases (*Bc*x) in terms of equilibrium fluctuations and apo and holo forms were decomposed

respectively into preassigned numbers of quasi-rigid bodies in range of two to seven. Within the intervening residues between the quasi-rigid bodies in each clustering number (Table 3 and Table 4), the commonly detected residues over four clustering modes in the two structures were identified as the hinge regions (represented in bold in Table 3 and Table 4). These regions are regarded as hinge region within the conformational selection model [Ma et al., 2002] which assumes dynamically changing populations of molecules. On the other hand, from comparing substrate free and bound forms, relative movements of compact structural units are observed and the hinge regions are located at the boundary of the units. DynDom was run to detect domain (protein subunit) and hinge region (Table 5) using apo and holo forms of *Bacillus subtilis* xylanases (*Bs*x) which is identical with the target enzyme *Bc*x over 99% in terms of sequence and shows almost similar catalytic functionality with *Bc*x. The detected region is the hinge in terms of induced fit theory [Koshland, 1958]. Finally the four residue groups detected in the both viewpoints were selected as target hinge region (Table 6).

As previously described, hinge region is defined as a fixed boundary region between moving subunits, in the other word, the regions contains residues fluctuating less than neighboring motional residues do. FIRST 6.2 was run to estimate the fluctuation of each residue with default parameters except that the energy cutoff was set to -2.4 kcal/mol and the result is shown in Figure 3 and Table 7. In Figure 3, the continuous line represents the mean value of the residual

fluctuation of entire residue. The result shows that the means RMSD value of identified hinge region is relatively lower than that of entire residues. This indicates that the hinges were detected in the region neighboring largely moving subunits and the results accord with the definition of the hinge region.

Table 3. Boundary residues between the quasi-rigid bodies (Apo form)

Decomposition number	Boundary residues
2	43-44, **50-51**, 68-69, 81-82, 90-91, **134-135**, **143-144**, 167-168
3	41-42, **51-52**, 66-67, 70-71, 78-79, 84-85, 88-89, 110-111, 127-128, 137-138, **142-143**, **159-160**, 164-165, 168-169
4	7-8, 18-19, 27-28, 38-39, 43-44, **50-51**, 58-59, 64-65, 68-69, 70-71, 78-79, 83-84, 85-86, 87-88, 90-91, 109-110, 127-128, **135-136**, **143-144**, **159-160**, 164-165, 167-168, 170-171, 180-181
5	4-5, 8-9, 17-18, 27-28, 37-38, 41-42, 46-47, 47-48, 54-55, 58-59, 62-63, 65-66, 70-71, 78-79, 81-82, 84-85, 88-89, 90-91, 110-111, 127-128, **133-134**, 138-139, 139-140, 144-145, **159-160**, 164-165, 169-170, 172-173, 180-181
6	2-3, 9-10, 17-18, 28-29, 36-37, 45-46, **51-52**, 58-59, 63-64, 70-71, 79-80, 90-91, 110-111, 125-126, 127-128, **133-134**, 137-138, **142-143**, **159-160**, 165-166, 172-173, 179-180
7	2-3, 8-9, 17-18, 27-28, 37-38, 42-43, 46-47, **50-51**, 58-59, 64-65, 69-70, 79-80, 81-82, 85-86, 90-91, 110-111, 126-127, **134-135**, **143-144**, **159-160**, 167-168, 171-172, 179-180

Table 4. Boundary residues between the quasi-rigid bodies (Holo form)

Decomposition number	Boundary residues
2	43-44, **50-51**, 68-69, 81-82, 90-91, **134-135**, **143-144**, 167-168,
3	41-42, **51-52**, 66-67, 70-71, 78-79, 84-85, 88-89, 110-111, 127-128, 137-138, **142-143**, **159-160**, 164-165, 168-169
4	7-8, 18-19, 27-28, 38-39, 43-44, **50-51**, 58-59, 64-65, 68-69, 70-71, 78-79, 83-84, 85-86, 87-88, 90-91, 109-110, 127-128, **135-136**, **143-144**, **159-160**, 164-165, 167-168, 170-171, 180-181
5	4-5, 8-9, 17-18, 27-28, 37-38, 41-42, 46-47, 47-48, 54-55, 58-59, 62-63, 65-66, 70-71, 78-79, 81-82, 84-85, 88-89, 90-91, 110-111, 127-128, **133-134**, 138-139, 139-140, 144-145, **159-160**, 164-165, 169-170, 172-173, 180-181
6	**3-4**, 8-9, **17-18**, **28-29**, 37-38, 43-44, 49-50, 55-56, **58-59**, **62-63**, **65-66**, 68-69, 80-81, 81-82, **84-85**, **88-89**, 90-91, **109-110**, **110-111**, 126-127, **128-129, 133-134**, 134-135, **144-145**, 159-160, 166-167, **170-171, 172-173,** 179-180
7	**3-4**, 9-10, **17-18**, 25-26, 27-28, **28-29**, 36-37, 41-42, **51-52**, **58-59**, 59-60, **62-63**, **65-66**, 66-67, 69-70, 79-80, **84-85**, **88-89**, 91-92, **109-110, 110-111,** 125-126, **128-129,** 130-131, 132-133, **133-134**, 136-137, **142-143**, 147-148, 158-159, 165-166, 168-169, **170-171**, **172-173**, 173-174, 174-175, 179-180, 180-181

Table 5. Hinge residues of *Bsx* predicted by DynDom

Hinge region	43-44 49-50 68-69 80-81 90-91 129-130 144-145 150-151 159-160 166-167

Table 6. Identified hinge residues

Position in *Bcx*	**Identified by PiSQRD**	**Identified by DynDom**
Finger (Back of hand)	50-51	49-50
Between thumb and finger (Near thumb)	127-128	129-130
Between thumb and finger (Near finger)	143-144	144-145
Between helix and finger	159-160	166-167

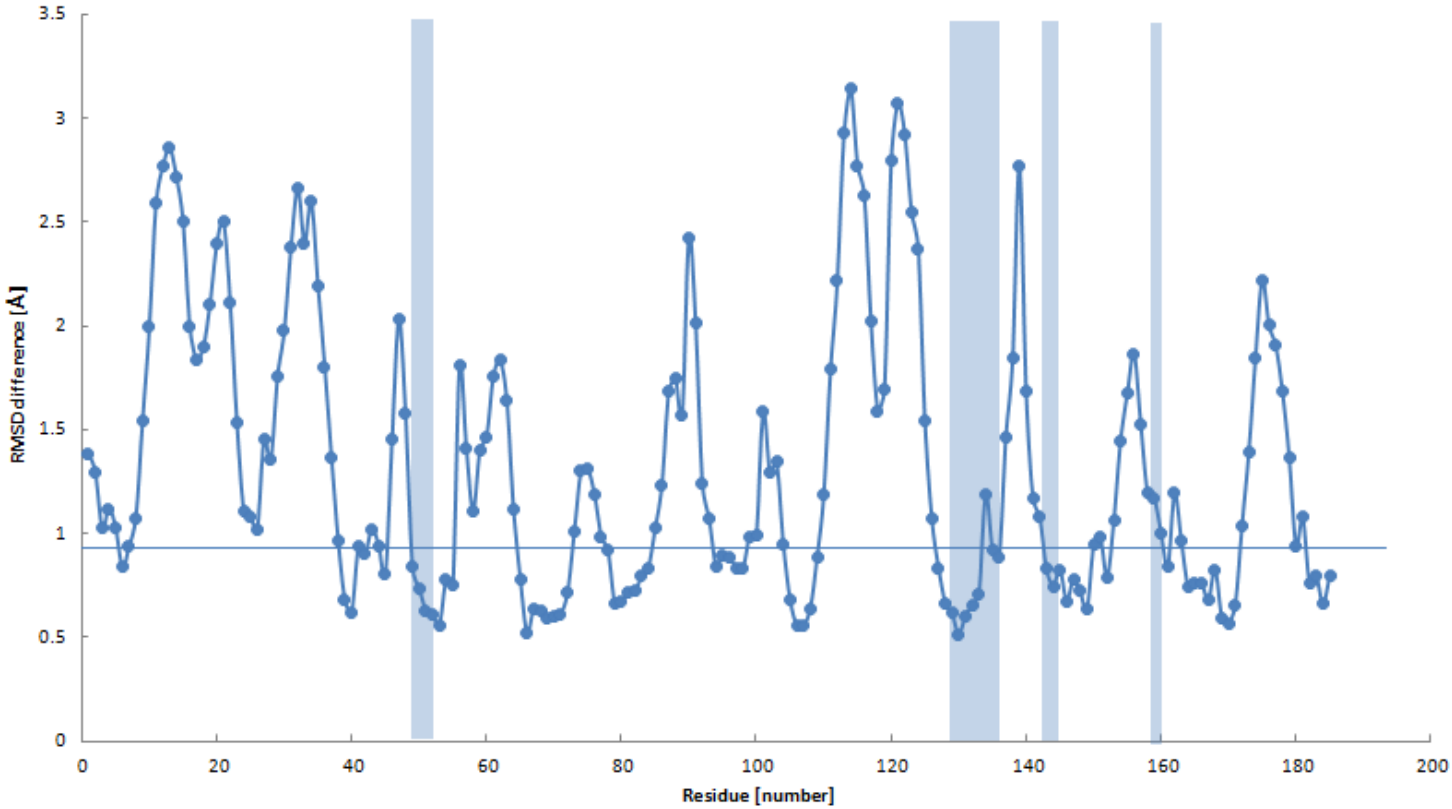

Figure 3. Residual fluctuation calculated by PRODA. The colored parts are the hinge regions, 49-51, 129-135 and 142-145, 159-160 from left to right.

Table 7. Residual fluctuation calculated by PRODA

Structure	Average of entire residue [Å]	Average of hinge region [Å]	Minimum [Å]	Maximum [Å]
Apo	1.32	0.893	0.517	3.14
Substrate bound	1.46	1.27	0.584	4.51

4.2. Selection of the target sites and mutations

Selection of the target hinge for the analysis was carried out by a case-specific investigation on the model enzyme, *Bc*x.

In the four hinge regions (Table 6, Figure 4) identified by the computational tools, Arg49 in the hinge region 49-53 (R49N, R49E, R49Q) and His156 near the region 159-160 (H156V) were previously investigated [Joo, 2011, Kim et al., 2012] (Table 8) by kinetic analysis. The remained hinge regions 129-135 and 141-145 which are located between thumb and finger region are selected for further study. In the two hinge regions, Val131, Arg132 and Asn141, Ala142 were chosen since the residues are located at the edges of the secondary structure, which could be mechanical hinge [Hayward, 1999] and are considered not to disrupt the protein structure correlated with its functional activity. As shown in Figure 4, the residues are located in the connecting region of the two atomic clusters containing catalytic residues (Glu78, Glu172) respectively, which indicates that the residues are located in the hinge region.

To investigate amino acid flexibility and the activity relationship, the target sites Val131, Arg132, Asn141 and Ala142 were mutated to several amino acids; Val131 to Ser; Arg132 to Met and Leu; Asn141 to Gly, Thr and Val; Ala142 to Ile. The reason the above amino acids were used to substitute the residues is that the residue flexibilities are differ from the original residue according amino acid B-

factor profile (Table 1) and that the intensity of interactions of the residue are changed by the mutation as a result of *in silico* mutation in terms of the kind of the interaction or the distance of the atoms.

The mutants generated in the previous studies mutants (R49N, R49E, R49Q, H156V) are also carried out *in silico* mutation and the alterations of the intra-protein interactions were calculated using PIC (Table 10).

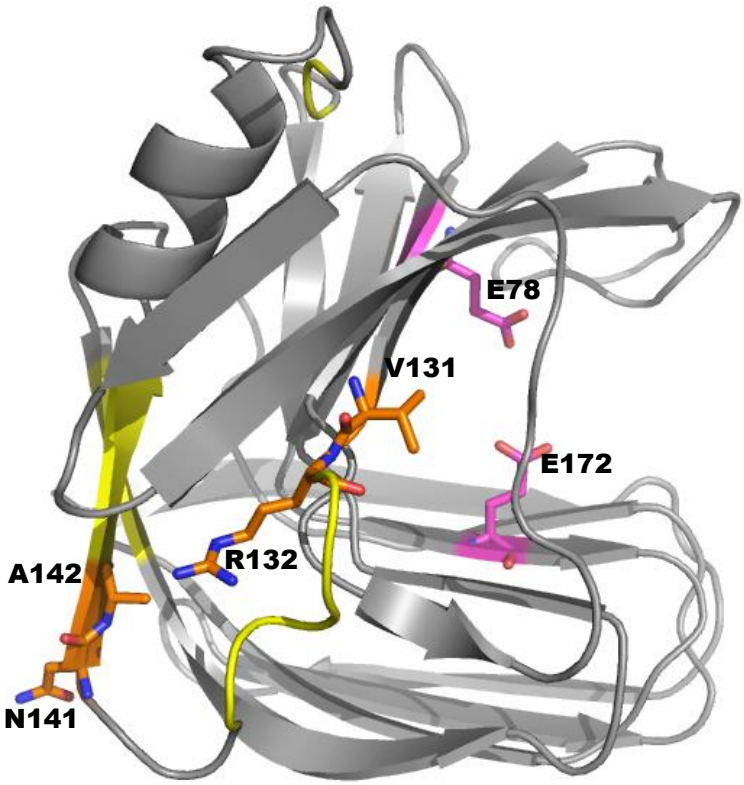

Figure 4. Target residues of *Bcx* (PDB: 1XNB). The hinge regions were in yellow, the target residues (V131, R132, N141, A142) are in orange and the catalytic residues (E78, E72) are in pink represented by stick diagram.

4.3. Characterization of mutants

In general, the enzyme activity is represented as Vmax (kcat) while the enzyme efficiency is represented as V_{max}/K_m which includes the binding affinity of an enzyme to a substrate. This research focuses on increasing the activity when an enzyme is reacting with excess substrate. For evaluation of the activity of wild type and the seven mutants, three of the hinge region 129-135 and four of the hinge region 141-145, the kinetic analysis was carried out and the V_{max} values were calculated by Lineweaver-Burk equation [Lineweaver et al., 1934] using the xylose standard curves generated in each substrate concentration (Table 9). As a result V_{max} of R132L, N141T, N141V and A142I were improved while those of V131S, R132L and N141G decreased or maintained.

Table 8. Relative values of the kinetic parameters (the previous study [Joo, 2011, Kim, 2012])

Hinge region	Enzyme	Rigidity[a]	V_{max}	K_m	V_{max}/K_m
-	Wild type	-	1	1	1
49-51	R49N	Flexible	1.20	0.69	2.04
	R49E	Flexible	0.70	0.74	1.13
	R49Q	Flexible	0.58	0.74	0.94
159-160	H156V	Rigid	1.19	0.65	1.70

[a] The flexibility of introduced amino acid compared to the original one according the amino acid B-factor profile (Table 1). “Flexible” (or “Rigid”) represents the more flexible (or rigid) amino acid than original one was introduced.

Table 9. Kinetic parameter values

Hinge region	Enzyme[a]	Rigidity[b]	V_{max} (mM/min)[C]	K_m (mM)[C]	V_{max}/K_m (1/min)[C]
-	Wild type	-	66.7	5.53	12.0
129-135	V131S	Flexible	31.3	2.78	11.2
	R132M	Rigid	75.2	5.51	13.6
	R132L	Rigid	45.7	2.49	18.3
141-145	N141G	Flexible	64.1	5.56	11.5
	N141T	Rigid	90.9	6.73	13.5
	N141V	Rigid	131	15.6	8.45
	A142I	Rigid	75.8	6.27	12.1

[a] The same concentration of enzymes (100ng/mL) was used for kinetic analysis

[b] The flexibility of introduced amino acid compared to the original one according the amino acid B-factor profile (Table 1.) “Flexible” (or “Rigid”) represents the more flexible (or rigid) amino acid than original one was introduced.

[c] Because beechwood xylan is a polymeric substrate, the substrate concentration was transformed into product (xylose) concentration scale considering the weight concentration of substrate and molecular weight of xylose.

4.3.1. Hinge region between thumb and finger (near the thumb)

The hinge region 129-135 is located in the connecting site of the finger and the thumb of *Bc*x and the thumb which is known as the most flexible region in the enzyme and important for catalysis [Pollet et al., 2009]. In addition, this region is the most deformed atomic group in terms of RMSD value which occurs when the apo and the holo forms are superimposed. Near the hinge region, three mutants were generated V131S, R132M and R132L. In the case of Val131, the original amino acid Val is listed as a relatively rigid one in the amino acid B-factor profile (Table 1) and it can contribute to the rigid structure by forming hydrophobic interactions. This site was substitute to Ser which is more flexible than Val. In addition, the Val131 lost all of the five hydrophobic interactions (Table 11) in the result of *in silico* mutation (Figure 5), which implies that the rigidity of the residue maintained by hydrophobic interactions decreased, therefore, it is estimated that the flexibility increased after the substitution. In the experimental result of V131S, V_{max} decreased to 47% of that of wild type. The reason is considered that the mobility and flexibility of the thumb region increased since the constraint by hydrophobic interactions were broken and the increased mobility might hamper the closure of the active site pocket after the substrate binding, which is important for catalysis by prevention of water entering. In the case of Arg132, Arg is listed in relatively flexible side in the flexibility index and is also known as a flexible amino acid because of its long side chain. This site

was substitute to Met and Leu, both are relatively more rigid than the original one and can create hydrophobic interactions. In the results of *in silico* mutations, new hydrophobic interactions was generated in the both substitutions (Figure 6) (Table 11), which implies that the rigidity of the site 132 might be intensified, however, the cation-pi interaction was broken in R132L, which might weaken the rigidity. The experimental results of R132M and R132L showed 113 % and 69% of the wild type V_{max} respectively. The both substituted amino acids might create the hydrophobic interaction but the V_{max} of R132M increased while that of R132L decreased. The assumable reasons are that the shape of the amino acid and the loss of the cation-pi interaction. The side chain of Met is the simple line, which is similar with the original amino acid Arg, on the other hand, the shape of Lue is branched. The branched side chain could make broad atomic surface, which might lead collisions with the neighboring amino acids. Besides, the substitution might disrupt the cataion-pi interaction with Tyr105 and this is considered to create negative affects in the thumb fluctuation, thus activity.

4.3.2. Hinge region between thumb and finger (near the finger)

The hinge region 141-145 is located in the bended β-strand connecting the two atomic groups which contain each catalytic glutamic acid respectively. At the edge of the β-strand each site directed mutagenesis N141G, N141T, N141V and A142I was carried out. In the case of the target site N141, among the substitution amino acids of Ans141, Gly is a more flexible amino acid on the other hand Thr and Val are more rigid ones than Asn (Table 1). From the result of *in silico* mutation (Figure 7) and protein interactions calculator (PIC), in N141G and N141T there did not occur any interaction changes in terms of the number or the kind whereas the hydrophobic interaction with Trp185 occurs in N141V. However when N141G and N141T were investigated structurally in the mutant N141M there is possibility of new hydrogen bond formation because the distance between the hydrogen atom in the side chain of Met and the oxygen of Asn54 is 3.4Å. In contrast, in the mutant N141A there is little possibility of new interaction occurring because of its short side chain. Although a hydrogen bond is relatively weak interaction, it has a critical role in protein folding and its strength is proportional to the numbers and inversely proportional to the distance between the atoms forming hydrogen bond [Jeffrey, 1997]. Therefore, it is estimated that N141G induces more flexible region than the other mutants in which new interactions could be added. Experimental results show that V_{max} of N141G is almost same with that of wild type whereas V_{max} of N141T and N141V increased

to 136% and 196% respectively (Table 9). The reason of increased V_{max} might be related with the structural rigidity of the region introduced by additional hydrogen bonds or hydrophobic interaction. In the case of Ala142 (Figure 8), the residue was substituted to more rigid amino acid Ile, which might add a hydrophobic interaction and this indicates that the local structural rigidity increased. From the experimental result, the mutant showed 113% V_{max} of the wild type. The tendency is observed that the V_{max} enhanced mutants were substituted to amino acid which leads to more rigid local structure.

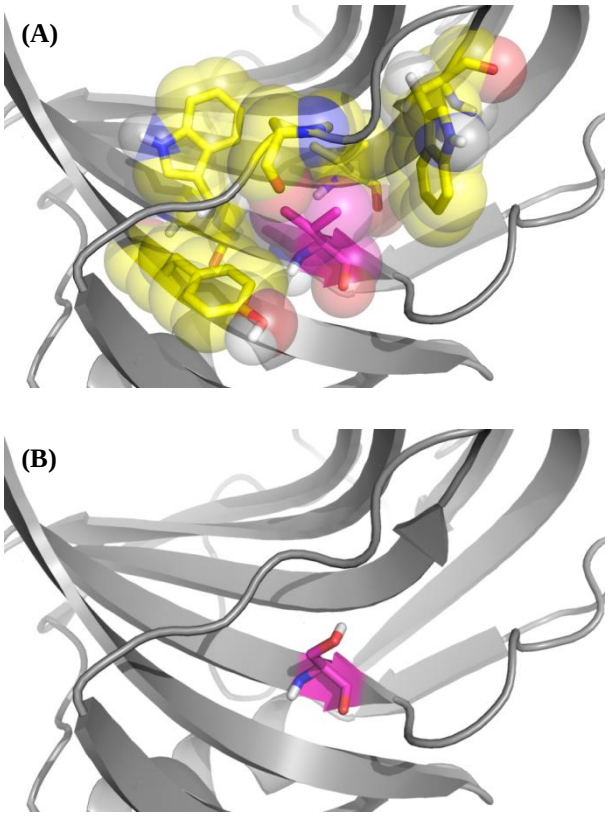

Figure 5. *in silico* mutation results of the target site Val131. (A) The wild-type representing Val131 representing hydrophobic interactions with other residues. (B) Mutant V131S with missed hydrophobic interactions.

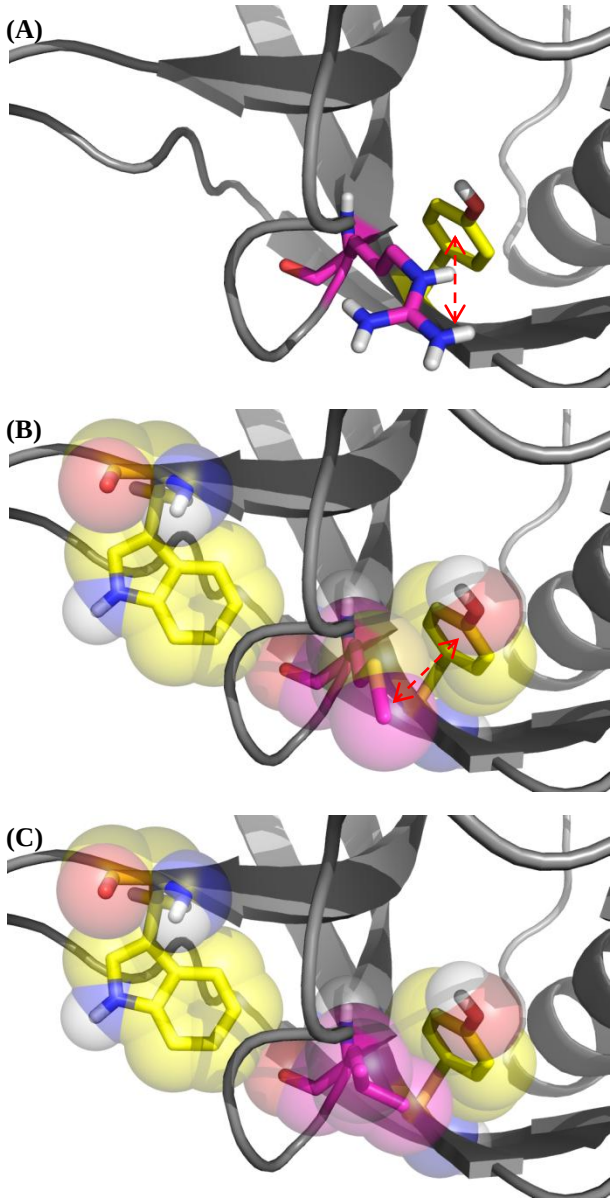

Figure 6. *in silico* mutation results of the target site Arg132. (A) The wild-type representing Arg132 with cation-pi interaction with Tyr105. (B) Mutant V131M representing aromatic-sulphur interaction with Tyr105 and hydrophobic interaction with Trp85. (C) Mutant V131L representing hydrophobic interaction with Trp 85 and missed cation-pi.

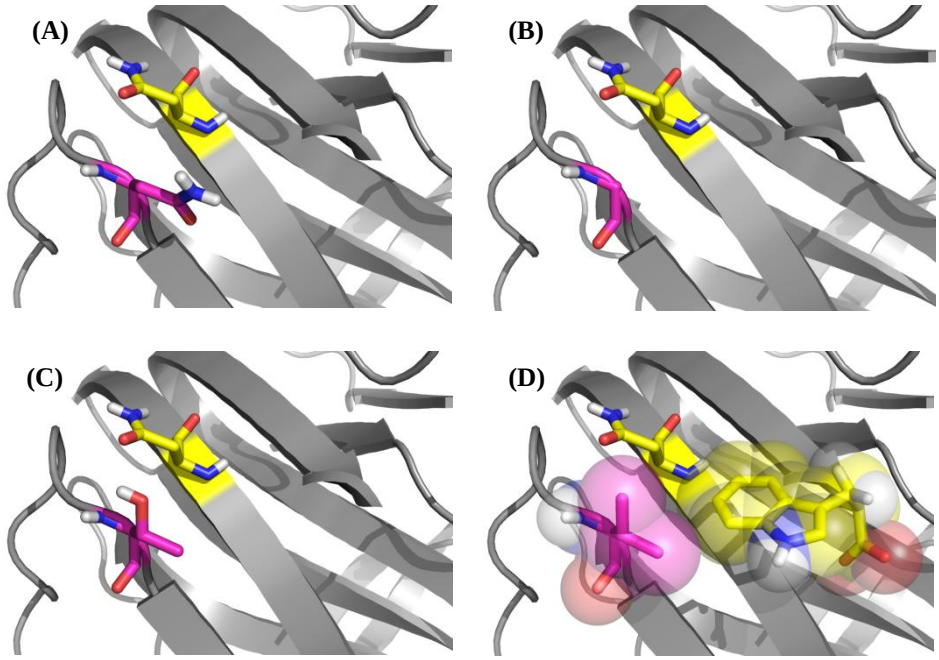

Figure 7. *in silico* mutation results of target sites Asn141. (A) The wild-type representing Asn132 with cation-pi interaction with Tyr105. (B) Mutant N141G. (C) Mutant N141T. (D) Mutant N141V representing hydrophobic interaction with Trp185.

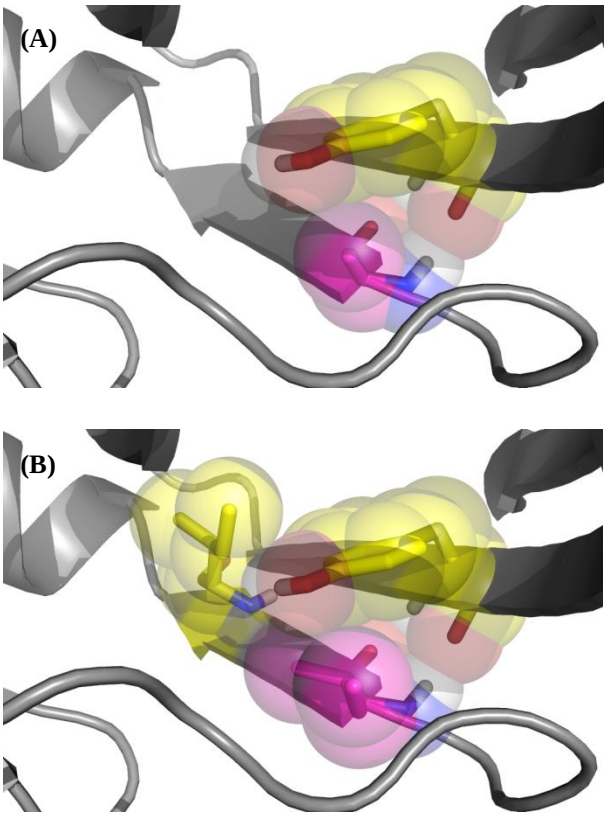

Figure 8. *in silico* mutation results of the target site Ala142. (A) The wild-type representing Ala131 representing hydrophobic interactions with Tyr53. (B) Mutant V142I adding hydrophobic interaction with I142.

Table 10. Intra-protein interactions of wild-type and mutants calculated by PIC (Analysis of the previous study)

Enzyme	Hydro-phobic interact-tion	Intra-protein hydrogen bond			Additional interaction
		Main chain - Main chain	Main chain - Side chain	Side chain - Side chain	
WT(49)		F146(N)-R49(O)	R49(NH1)-T44(O)	R49(NE)-Q167(OE1)	W42-R49 (Cation-pi)
R49N		F146(N)-N49(O)	S46(N)-N49(ND2)	N49(ND2)-Q167(OE1) Q167(OE1)-N49(ND2)	
R49E		F146(N)-E49(O)	S46(N)-E49(OE2) E49(OE2)-T44(O)	E49(OE1)-Q167(OE1)	
R49Q		F146(N)-Q49(O)	S46(N)-Q49(NE2) Q49(NE2)-T44(O)	Q49(OE1)-Q167(OE1) Q49(NE2)-Q167(OE1)	
WT (156)		H156(N)-A152(O) H156(N)-W153(O) H156(N)-K154(O) M158(N)-H156(O)	H156(NE2)-K95(O) H156(ND2)-A152(O)		
H156V	I107-V156 W153-V156 V156-M158	V156(N)-A152(O) V156(N)-W153(O) V156(N)-K154(O) V158(N)-H156(O)			

Table 11. Intra-protein interactions of wild-type and mutants calculated by PIC

Enzyme	Hydrophobic interaction	Intra-protein hydrogen bond		Additional interaction
		Main chain - Main chain	Main chain - Side chain	
WT(131)	V82-V131 W85-V131 P90-V131 Y108-V131 W129-V131	N106(N)-V131(O) V131(N)-N106(O) Q133(N)-V131(O)	R89(NH1)-V131(O)	
V131S		N106(N)-S131(O) S131(N)-N106(O) Q133N(N)-S131(O)	R89(NH1)-S131(O)	
WT(132)		R132(N)-V82(O) S134(N)-R132(O)	R89(NE)-R132(O) R89(NH1)-R132(O) R132(NH2)-S134(O)	Y105-R132 (Cation-Pi interaction)
R132M	W85-M132 Y105-M132	M132(N)-V82(O) S134(N)-M132(O)	R89(NE)-M132(O) R89(NH1)-M132(O) R136(N)-M132(SD)	Y105-M132 (Aromatic-Sulphur Interactions)
R132L	W85-L132 Y105-L132	L132(N)-V82(O) S134(N)-L132(O)	R89(NE)-L132(O) R89(NH1)-L132(O)	

Table 11. Continued.

Enzyme	Hydrophobic interaction	Intra-protein hydrogen bond		Cation-Pi interaction
		Main chain - Main chain	Main chain - Side chain	
WT(141)			N141(N)-N54(OD1)	
N141G			G141(N)-N54(OD1)	
N141T			T141(N)-N54(OD1)	
N141V	V141-W185		V141(N)-N54(OD1)	
WT(142)	Y53-A142	Y53(N)-A142(O) A142(N)-Y53(O) A142(N)-S140(O)		
A142I	Y53-I142 I142-I144	Y53(N)-I142(O) I142(N)-Y53(O) I142(N)-S140(O)		

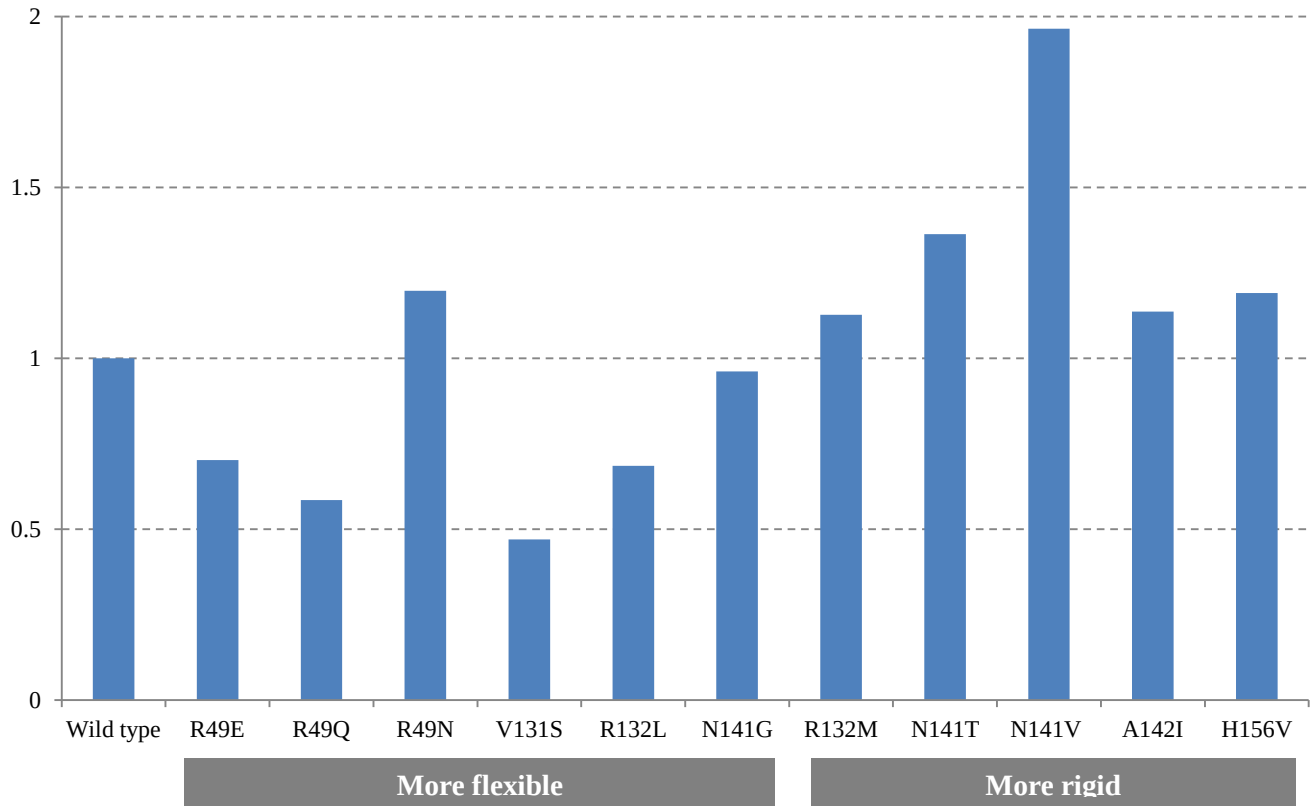

Figure 9. Relative V_{max} values of wild type and all mutants of the previous and this study. "More flexible" (or "More rigid") represents the alteration in the flexibility of the mutated residue in terms of the intra-protein interactions.

4.4. Overall discussion

The hinge residues identified by several computational based tools using apo and substrate bound forms are located in the region connecting the amino acid cluster which deforms most by substrate binding or which contains catalytic residue. It indicates that identification of meaningful hinge region might be carried out using public programs without a lot of crystallographic structures or information of other proteins in the same family.

Out of seven mutants newly generated in the detected hinge region V131, R132, N141 and A142, four mutants showed increased V_{max} and the V_{max} of the rest was maintained or decreased (Figure 10). From the experimental results the tendency was observed between the V_{max} and the level of flexibility in terms of amino acid B-factor profile or committed interactions of substituted amino acids. That is the V_{max} decreased mutants V131S, R132L and N141G were mutated to more flexible amino acids than the original one or lost intra-protein interactions, on the other hand, more rigidly substituted mutants increased V_{max}. In other words mutation to the more rigid amino acid might be related with the V_{max} enhancement. The results of previous mutational study (R49E, R49Q, H156V) contribute to the confirmation of the tendency (Figure 10). For further investigation for revealing the cause of V_{max} enhancement, it is required that temperature dependant kinetic parameter for calculating activation energy which

is related with V_{max} value in catalytic coordination.

Contrary to V_{max} enhancement, V_{max} improved mutants worsen their substrate binding represented by K_m value. The first reason might be that though substitution to more rigid amino acid allowed maintaining the conformation for catalysis after substrate binding, it could not induce the freedom for substrate binding. The other reason is specified to N141, where is revealed as a secondary binding site, which leads to enhance substrate affinity, thus increased activity, in cooperation with the active site [Ludwiczek et al., 2007]. The reason of worsened substrate binding might be the negative modulation of the secondary binding site.

5. Conclusion

In this study the hinge region was identified efficiently using computational tool and the relationship between the hinge flexibility and the enzyme activity was investigated by site-directed mutagenesis. Hinges in enzymes play a role as a connector of quasi-rigid bodies which fluctuate in a concerted residual group and the flexibility of the hinge might influence the quasi-rigid body motions, which is related with catalysis. The relationship between hinge flexibility and activity was investigated using model enzyme *Bacillus circulans* xylanase which shows hinge bending motions during catalysis. Two computer programs were run to identify the hinge and the regions coincidentally identified by the both programs were selected. In the identified hinge regions, the target residues for mutations V131, R132, N141 and A143 were selected not to disrupt the structure and catalytic functionality. The residues were mutated to alter the flexibility according to amino acid B-factor profile and the intensity of interactions. Val131 and R132 are located in and near the edge of β-strand of the most flexible thumb region in *Bc*x and the mutant substituted to more flexible amino acid showed decreased V_{max} (V131S) whereas the mutant substituted to more rigid amino showed increased V_{max} (R132M). Asn141 and Ala142 in the connector between two quasi-rigid bodies containing catalytic residues respectively was mutated to several amino acids (N141G, N141T, N141V, A142I). From kinetic analysis it is revealed that the V_{max} tends to increase along with rigidity of the hinge region. The analysis of

the mutants (R49E, R49Q, H156V) which were generated in the previous study confirms the tendency. The reason might be that the hinge region acts as a support of the structure after the substrate binding, which aids the catalysis properly. In conclusion, from investigation of *Bc*x hinge regions it is figured out that the rigidity of hinge region acts positively in the enhancement of V_{max}.

References

Bradford, M. M., A rapid and sensitive method for the quantitation of microgram quantities of protein utilizing the principle of protein dye binding, Analytical Biochemistry, 72, 248-254, 1976

Brooks, C. L. III, Karplus, M. and Pettitt, B. M., Protein Structure and Dynamics—An Overview, Advances in Chemical Physics: Proteins: A Theoretical Perspective of Dynamics, Structure, and Thermodynamics, 71, 7-21, 1998

Coughlan, M. P., Hazlewood, G. P., β-1, 4-D-xylan-degrading enzyme systems: biochemistry, molecular biology and applications, Biotechnology and Applied Biochemistry., 17, 259–289, 1993

Fischer, E., Einfluss der Configuration auf die Wirkung der Enzyme, Berichte der deutschen chemischen Gesellschaft, 27, 3, 2985–2993, 1894

Fisher, C. L., and Pei, G. K., Modification of a PCR-based site-directed mutagenesis method, Biotechniques, 23, 570-574, 1997

Hammes-Schiffer, S., Impact of Enzyme Motion on Activity, Biochemistry, 41,

45, 13335–13343, 2002

Hammes, G. G., Multiple conformational changes in enzyme catalysis, Biochemistry, 41, 8221-8228, 2002

Hayward, S. and Berendsen H. J., Systematic analysis of domain motions in proteins from conformational change: New results on citrate synthase and T4 lysozyme, PROTEINS: Structure, Function, and Genetics, 30, 144-154, 1998

Hayward, S. and Lee, R. A., Improvements in the analysis of domain motions in proteins from conformational change: DynDom version 1.50, Journal of Molecular Graphics and Modelling, 21, 3, 181–183, 2002

Hayward, S., Structural principles governing domain motions in proteins, PROTEINS: Structure, Function, and Genetics, 36, 425-435, 1999

Jeffrey, G. A., An introduction to hydrogen bonding, Oxford University Press, 1997

Joo, J. C. and Yoo, Y. J., Computational enzyme design based on flexibility analysis for improving stability and activity, Seoul National University Library, 10101419035, 2011

Kim, K. S., Fuchs, J. A., Woodward, C.K., Hydrogen exchange identifies native-state motional domains important in protein folding, Biochemistry, 21, 32, 37, 9600–9608, 1993

Kim, T. H., Joo, J. C and Yoo, Y. J., Hydrophobic interaction network analysis for thermostabilization of a mesophilic xylanase, Journal of Biotechnology, 161, 1, 49-59, 2012

Koshland, D.E., Application of a theory of enzyme specificity to protein synthesis, Proceedings of the National Academy of Sciences of the United States of America, 44, 98-104, 1958

Krivov, G. G., Shapovalov, M.V., Dunbrack, R. L. Jr., Improved prediction of protein side-chain conformations with SCWRL4. PROTEINS: Structure, Function, and Genetics, 77, 4, 778-95, 2009

Lineweaver, H. and Burk, D., The determination of enzyme dissociation constants, Journal of the American Chemical Society, 56, 3, 658–666, 1934

Ludwiczek, M. L., Terrence Kantner, M. H. and McIntosh, L. P., A secondary xylan-binding site enhances the catalytic activity of a single-domain family 11 glycoside hydrolase, Journal of Molecular Biology, 373, 2, 337-354, 2007

Ma, B., Shatsky, M., Wolfson H. J. and Nussinov R, Multiple diverse ligands binding at a single protein site: A matter of pre-existing populations, Protein Science, 11, 184-197, 2002

Muilu, J., Torronen, A., Perakyla, M. and Rouvinen J., Functional conformational changes of endo-1, 4-xylanase II from *Trichoderma reesei*: A molecular dynamics study, PROTEINS: Structure, Function, and Genetics, 31, 434-444, 1998

Neet, K. E., Enzyme catalytic power minireview series, The Journal of Biological Chemistry, 273, 25527-25528, 1998

Pollet, A., Vandermarliere E., Lammertyn J., Strelkov S.V., Delcour J.A. and Courtin C. M., Crystallographic and acitivity-based evidence for thumb flexibility and its relevance in glycoside hydrolase family 11 xylanases, PROTEINS: Structure, Function, and Genetics, 77, 2, 395-403, 2009

Potestio, R, Pontiggia, F, Micheletti, C, Coarse-Grained Description of Protein Internal Dynamics: An Optimal Strategy for Decomposing Proteins in Rigid Subunits, Biophysical Journal, 96, 12, 4993-5002, 2009

Purmonen, M., Valjakka, J., Takkinen, K., Laitinen, T. and Rouvinen1, J.,

Molecular dynamics studies on the thermostability of family 11 xylanases, Protein Engineering, Design and Selection, 20,11, 551-559. 2007

Radivojac, P., Obradovic, Z., Smith, D. K., Zhu, G., Vucetic, S., Brown, C. J., Lawson, J. D., Dunker, A. K., Protein flexibility and intrinsic disorder, Potein Science, 13, 1, 71-80, 2004

Schramm, A. M., Mehra-Chaudhary, R., Furdui, C. M., and Beamer, L. J., Backbone flexibility, conformational change, and catalysis in a phosphohexomutase from *Pseudomonas aeruginosa*, Biochemistry, 47, 35, 9154–9162, 2008

Schulz, G., Domain motions in proteins, Current Opinion in Structural Biology, 1, 6, 883-888, 1991

Sime, J. T., Applications of biocatalysis to industrial processes, Journal of Chemical Education, 76, 12, 1999

Szabo, J., Varga, A., Flachner, B., Konarev, P. V., Svergun, D. I., Zavodszky, P. and Vas, M., Role of side-chains in the operation of the main molecular hinge of 3-phosphoglycerate kinase, FEBS Letters, 582, 9, 1335-1340, 2008

Tina, K. G., Bhadra, R. and Srinivasan, N., PIC: Protein Interactions Calculator, Nucleic Acids Research, 35, 5, 473-476, 2007

Tsuchiya, D., Shimizu, N., Tomita, M., Cooperativity of two active sites in bacterial homodimeric aconitases, Biochemical and Biophysical Research Communications, 379, 2, 485-488, 2009

Wells, S., Menor, S., Hespenheide, B. and Thorpe, M.F., Constrained geometric simulation of diffusive motion in proteins, Physical Biology, 2, 127-136, 2005

Yon, J. M., Perahia, D., Ghelis, C., Conformational dynamics and enzyme activity, Biochimie, 80, 33-42, 1998

Zheng, L., Baumann, U. and Reymond, J.L., An efficient one-step site-directed and site-saturation mutagenesis protocol, Nucleic Acids Research, 32, 14, e115, 2004

국문 요약

단백질인 효소는 여러 입체적 구조를 띠는 역동적 분자이며 이 역동성은 효소의 활성에 있어서 핵심적인 역할을 하는 것으로 알려져 있다. 효소의 여러 종류의 움직임들 중에서도 경첩(hinge)을 축으로 한 도메인들의 상대적인 움직임인 경첩 굽힘 움직임(hinge bending motion)이 효소의 물질 생성 속도와 크게 연관되어있다는 것과 이러한 움직임이 경첩 부분의 물리적 특성에 영향을 받고 있다는 보고에 주목하였다. 본 연구에서는 특히 경첩 부분의 유연성(flexibility)과 효소 활성의 관계를 이해하기 위해 효소의 구조적 분석을 통해 경첩 부분을 효율적으로 탐색하고 아미노산 치환을 통해 이 부분의 유연성을 조작하여 그 관계를 밝혀내고자 하였다. 대상 효소인 *Bacillus circulans* 자일라네이즈에 컴퓨터 프로그램을 적용하여 경첩을 탐색하고 얻어진 여러 경첩 지역 중, 구조적 관찰을 통해 효소 본래의 활성을 저해시키지 않도록 2차적으로 치환 후보 아미노산을 선택하여 그 유연성을 더욱 단단하게 하거나 유연하게 하는 돌연변이를 제작하였다. 그 결과 더욱 단단하게 치환한 힌지 구조에서 반응 속도(V_{max})가 올라가는 경향성을 찾을 수 있었고 최대 속도가 약 2배인 변이체를 확보할 수 있었다.

본 연구에서는 효소의 경첩 지역을 구조적 분석을 통하여 효율적으로 찾아내었고 그 유연성을 보다 단단하게 조작하는 것이

효소의 활성을 높이는데 기여하는 것을 밝혔다.

주요어: 단백질, 활성, V_{max}, 유연성, 경첩, 자일라네이즈

학번: 2010-23357